

Supporting Information for:

Mesoscopic superstructures of flexible porous coordination polymers synthesized *via* coordination replication

Kenji Sumida,^a Nirmalya Moitra,^b Julien Reboul,^a Shotaro Fukumoto,^b Kazuki Nakanishi,^b

Kazuyoshi Kanamori,^b Shuhei Furukawa,^{*a} and Susumu Kitagawa^{*a}

Structure and Flexibility of the Cu(bdc)(MeOH) and Cu(bdc)(bpy)_{0.5} Frameworks

The structure of the Cu(bdc)(MeOH) framework shown in Fig. S1 is one consisting of two-dimensional square grids consisting of dinuclear Cu²⁺ paddlewheels bridged by the bdc²⁻ ligands, with MeOH solvent molecules occupying the axial binding sites. The framework exhibits the reversible accommodation of guest molecules in the interlayer spaces, which results in a change in the distance between adjacent layers. The installation of bpy units results in the formation of the microporous Cu(bdc)(bpy)_{0.5} compound *via* the displacement of the coordinated MeOH molecules, which features an interpenetrated structure in which the pillars span the axial Cu²⁺ sites of every second layer such that the pillars are threaded through the cavities of the square grids. The Cu(bdc)(bpy)_{0.5} compound features a reversible transition between a closed phase in the evacuated state, to an open phase in the solvated state (see Fig. S2).

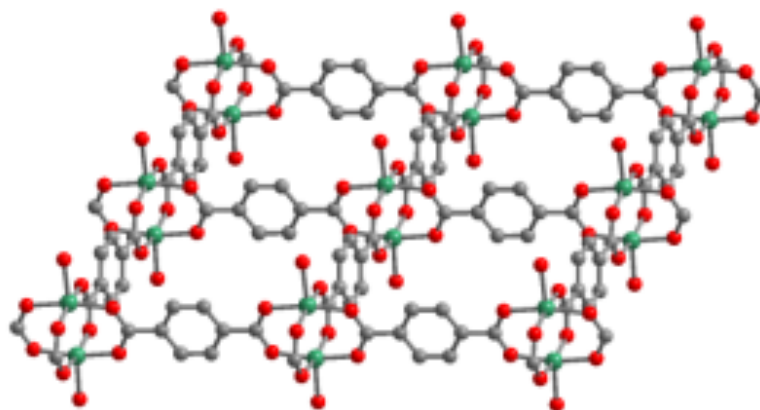


Fig. S1 A structural model showing a portion of the structure of the $\text{Cu}(\text{bdc})(\text{MeOH})$ compound. Green, gray and red spheres represent Cu, C and O atoms, respectively, while H atoms and the methyl group of the coordinated methanol molecules have been omitted for clarity.

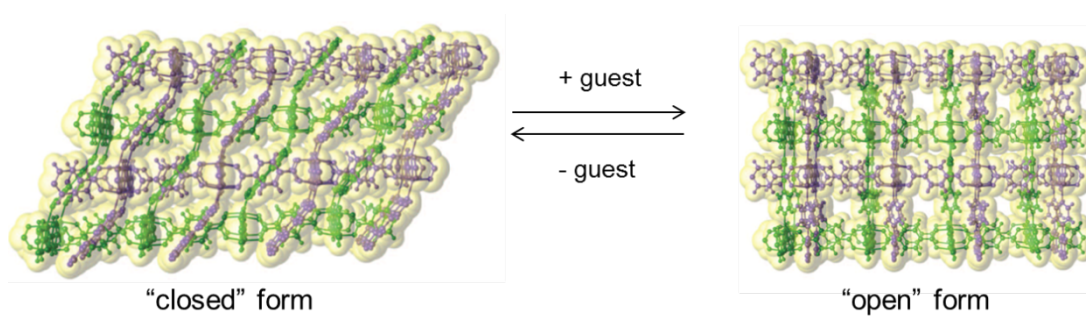


Fig. S2 Diagrams showing the interpenetrated structures of $\text{Cu}(\text{bdc})(\text{bpy})_{0.5}$ (purple and green), and the structural transition between closed and open pore forms upon guest inclusion and removal.

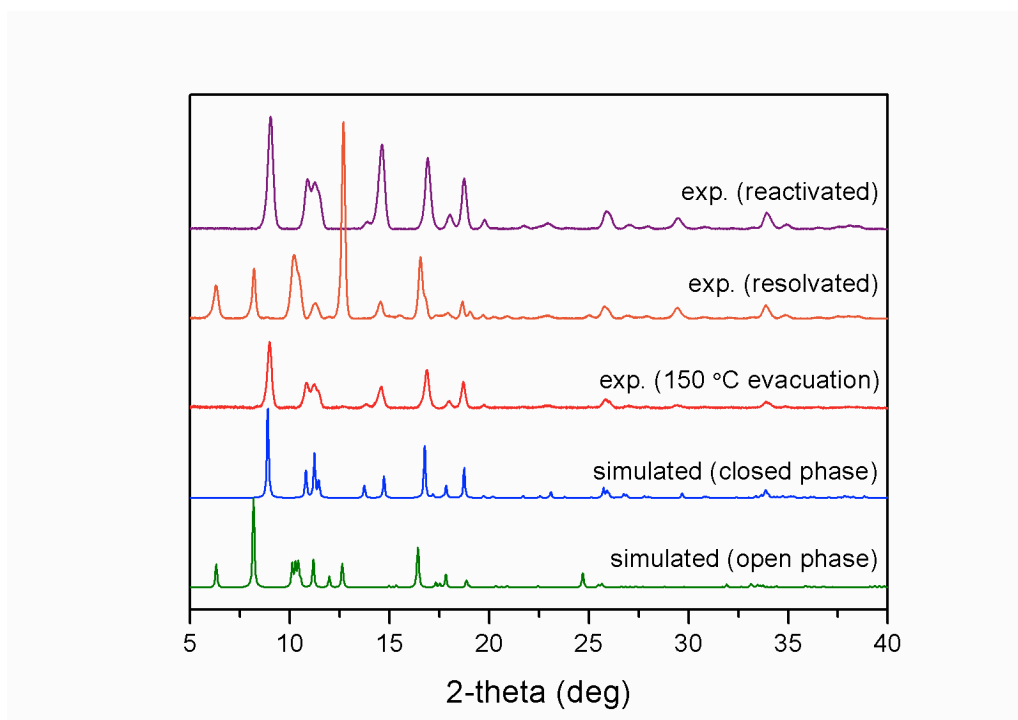


Fig. S3 Powder X-ray diffraction patterns as simulated for the open (green) and closed (blue) phases of $\text{Cu}_2(\text{bdc})_2(\text{bpy})$, and experimental data for a $\text{Cu}(\text{OH})_2$ -derived $\text{Cu}_2(\text{bdc})_2(\text{bpy})$ sample after 150 °C evacuation (red), resolution in methanol (orange), and reactivation at 150 °C (purple).

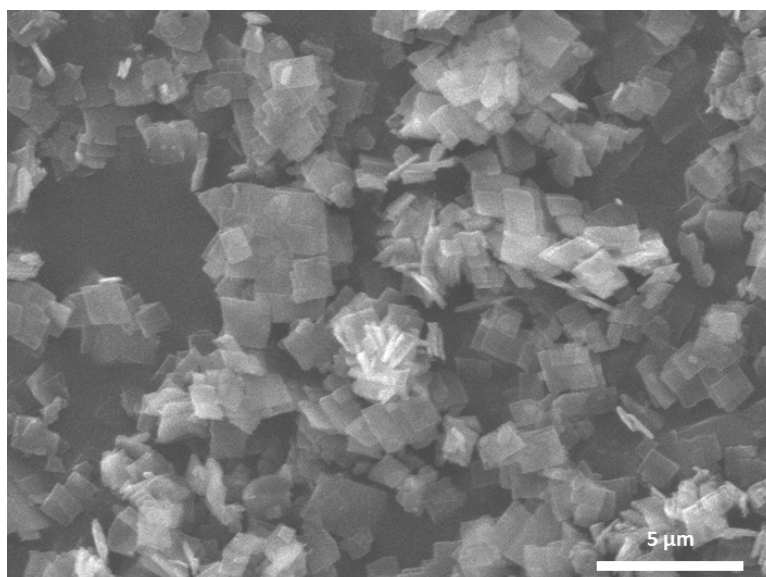


Fig. S4 An SEM of $\text{Cu}(\text{OH})_2$ -derived $\text{Cu}_2(\text{bdc})_2(\text{bpy})$, showing a thin, plate-like morphology.

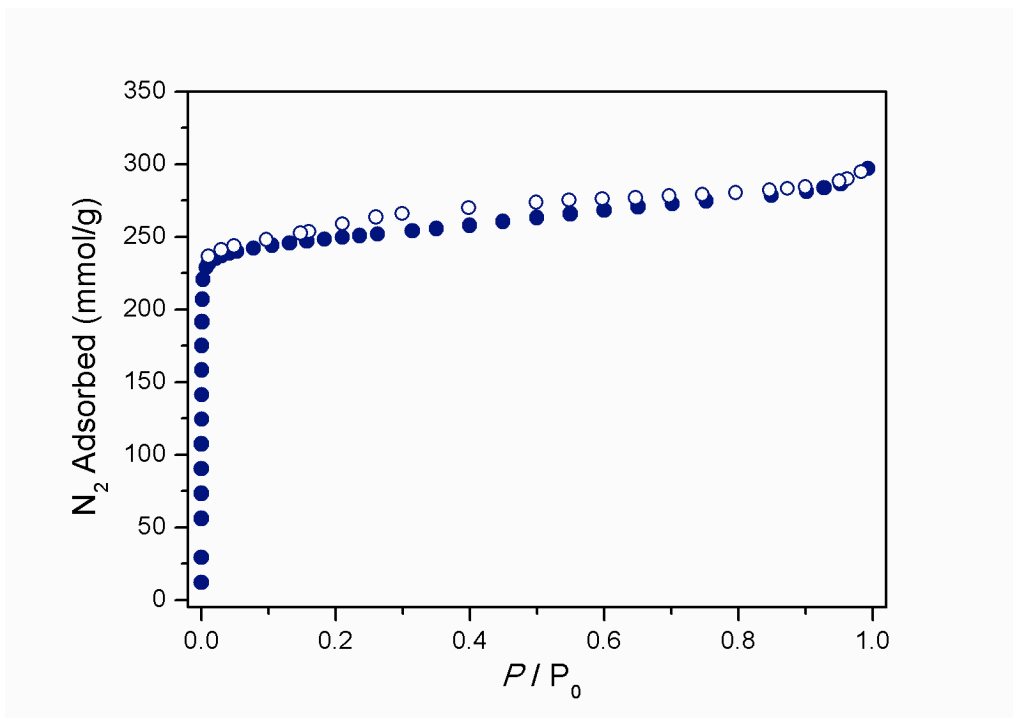


Fig. S5 N_2 adsorption data for $Cu(OH)_2$ -derived $Cu_2(bdc)_2(bpy)$ collected at 77 K. Closed and open symbols represent adsorption and desorption, respectively.

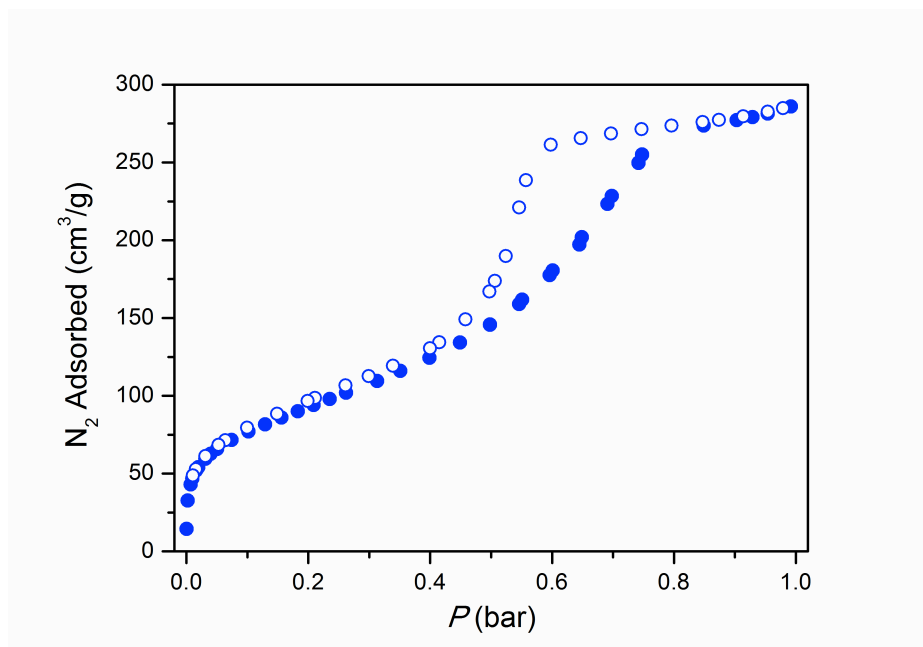


Fig. S6 N_2 adsorption data for the parent $Cu(OH)_2$ -PAAM composite collected at 77 K. Closed and open symbols represent adsorption and desorption, respectively.

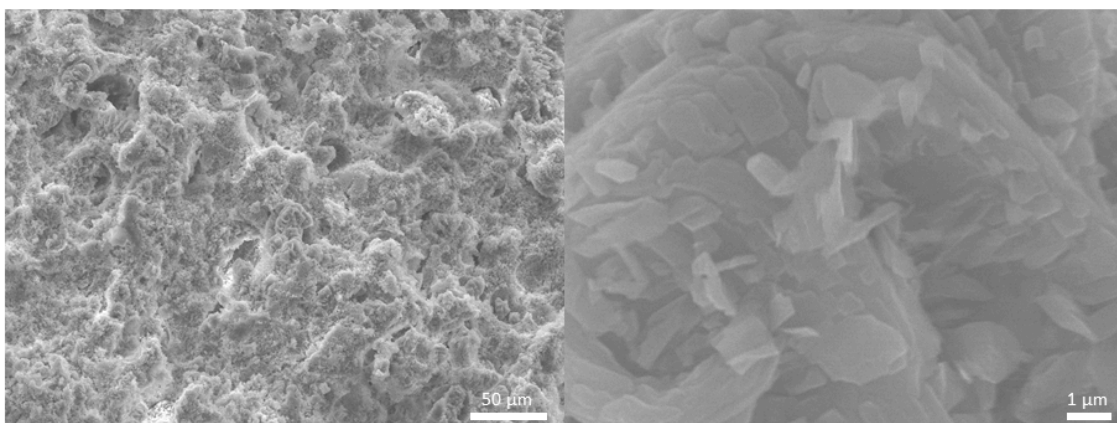


Fig. S7 SEM images of a cross section of a $\text{Cu}_2(\text{bdc})_2(\text{MeOH})_2$ monolith after replication showing a (left) a wide view and (right) a zoomed-in view.

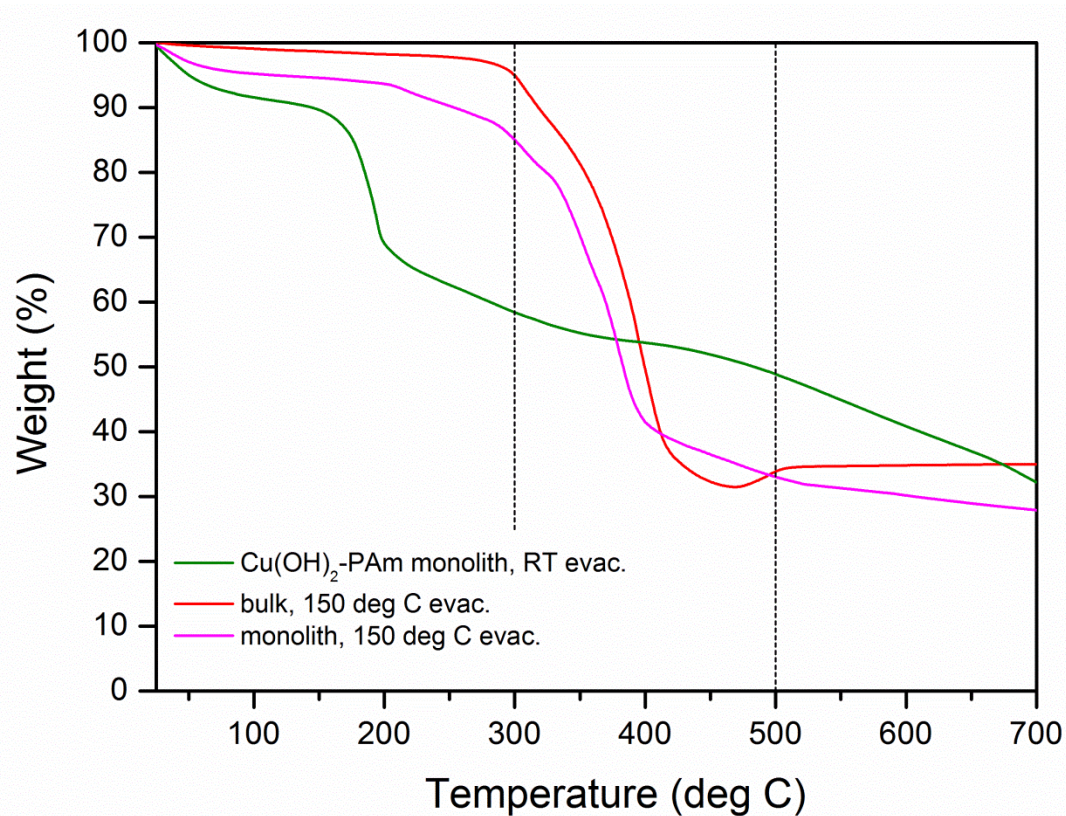


Fig. S8 Thermogravimetric data for the parent $\text{Cu}(\text{OH})_2$ -PAAm monolith (green), bulk $\text{Cu}(\text{bdc})(\text{MeOH})$ (red), and the $\text{Cu}(\text{bdc})(\text{MeOH})$ -PAAm monolith (pink) collected under an N_2 flow using a temperature ramp rate of 2 K/min. The dotted line represents the weight transition used to estimate the composition of the replicated monolith.

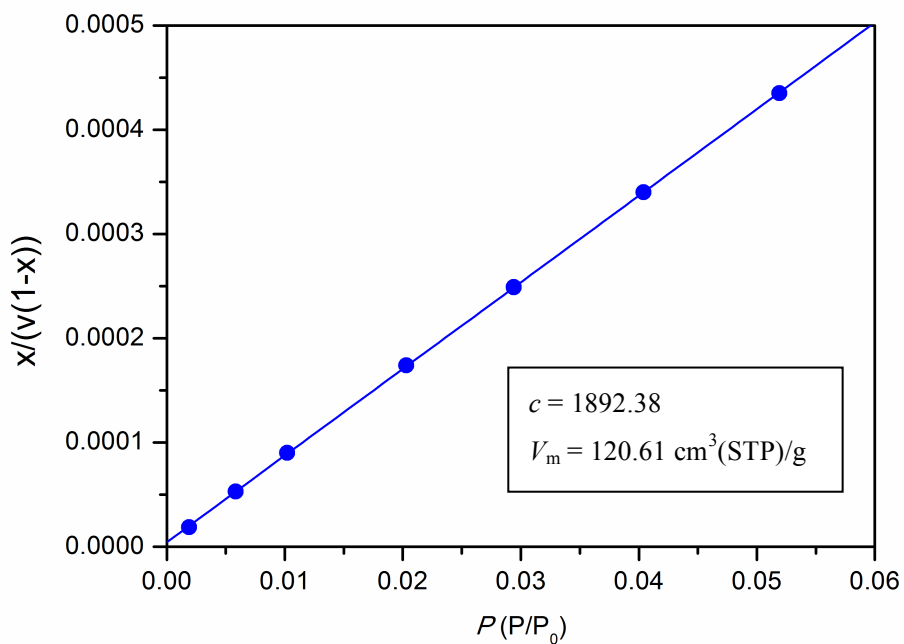


Fig. S9 A BET plot of the adsorption isotherm for N_2 in the $\text{Cu}(\text{bdc})(\text{MeOH})\text{-PAAm}$ monolith at 77 K, where x represents the quantity (P/P_0) and V is the volume of N_2 adsorbed. The blue line represents a linear best fit of the data points. Inset: parameters for the linear best fit and resulting constants for calculation of the BET surface area.

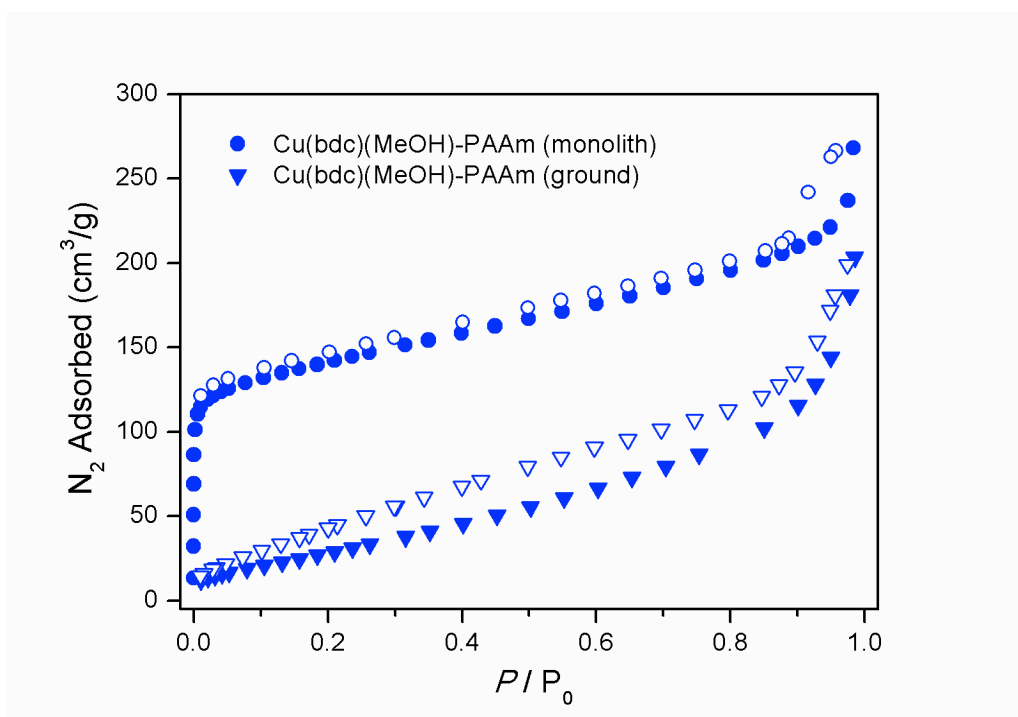


Fig. S10 N_2 adsorption data collected at 77 K for the $\text{Cu}_2(\text{bdc})_2(\text{MeOH})_2$ replicate in monolith form (circles) and after mechanical grinding (triangles). Closed and open symbols represent adsorption and desorption, respectively.

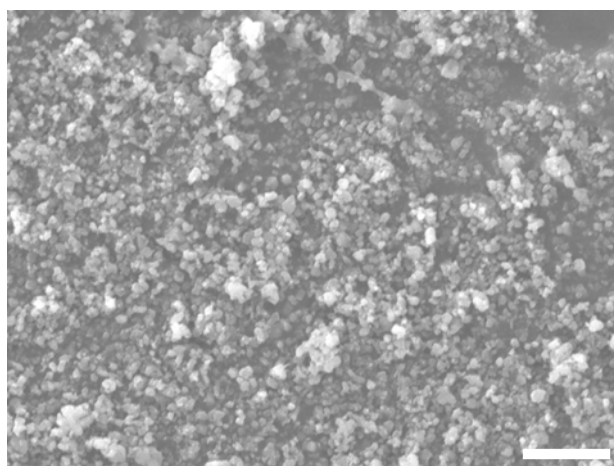


Fig. S11 Field-emission SEM image of the $\text{Cu}_2(\text{bdc})_2(\text{MeOH})_2$ monolith after mechanical grinding. The scale bar represents a distance of $10\ \mu\text{m}$.

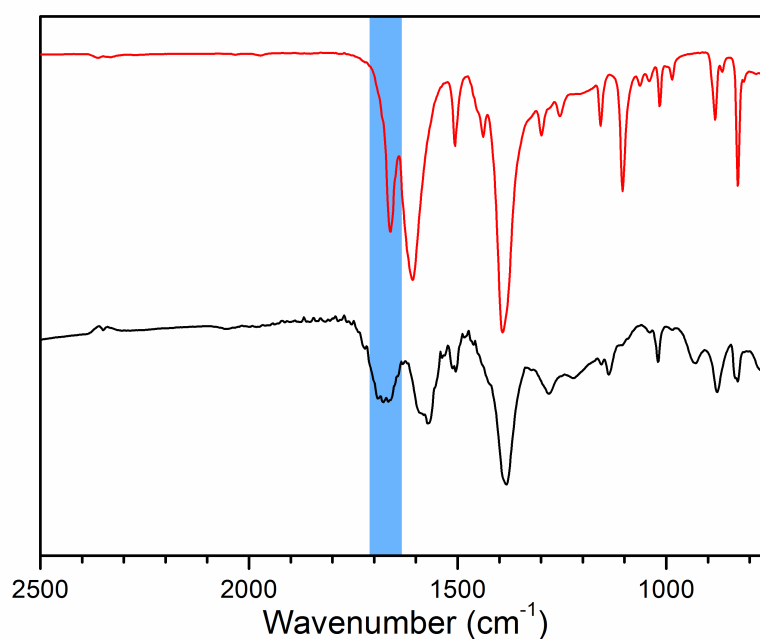


Fig. S12 Infrared spectra for a $\text{Cu}_2(\text{bdc})_2(\text{MeOH})_2$ monolith prepared by coordination replication (black), and a $\text{Cu}_2(\text{bdc})_2(\text{MeOH})_2$ powder prepared by reaction of a mechanically ground sample of the same parent phase (red). The shaded region indicates the amide C=O stretch, which reflects the presence of polyacrylamide within the sample.

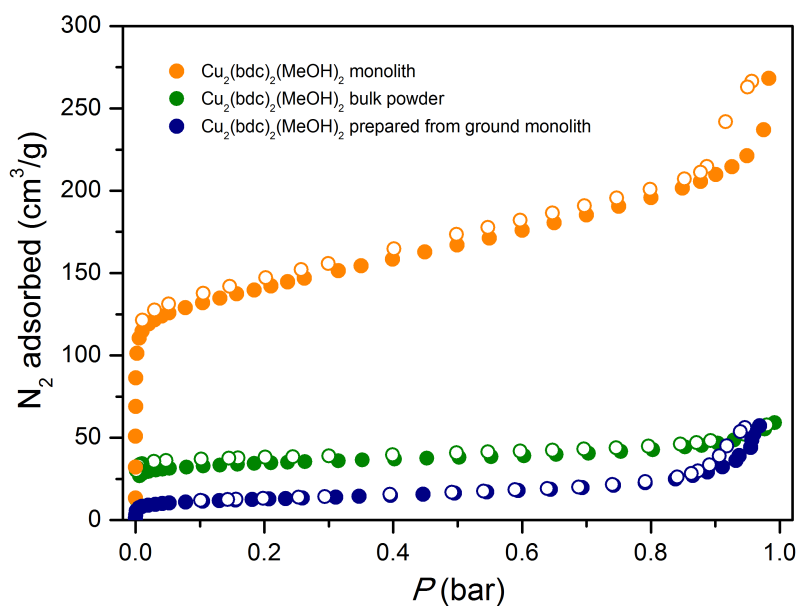


Fig. S13 N₂ adsorption isotherms collected at 77 K for a Cu₂(bdc)₂(MeOH)₂ bulk powder (green), a Cu₂(bdc)₂(MeOH)₂ monolith (orange), and a Cu₂(bdc)₂(MeOH)₂ powder sample prepared from a ground sample of the parent monolith (blue). Closed and open symbols represent adsorption and desorption data, respectively.

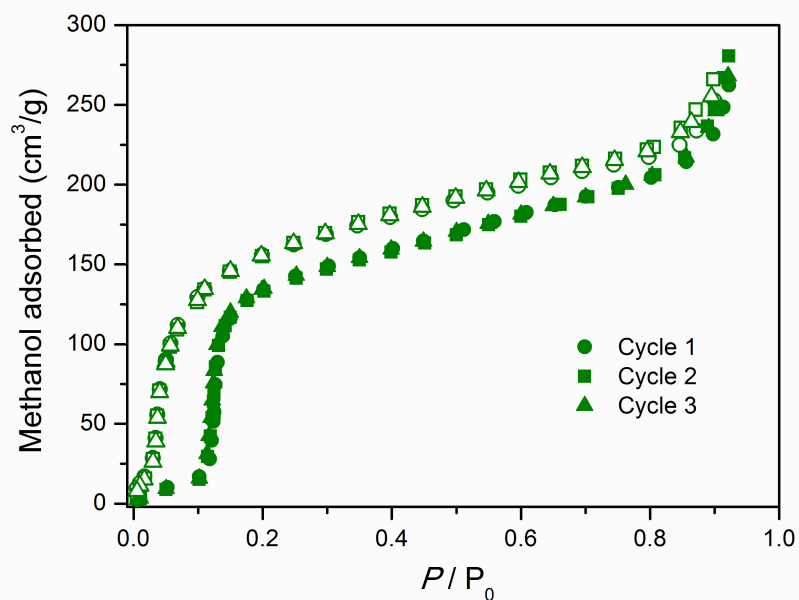


Fig. S14 MeOH adsorption data for a monolithic Cu₂(bdc)₂(bpy) replicate at 298 K for three adsorption and desorption cycles. Closed and open symbols represent adsorption and desorption, respectively.

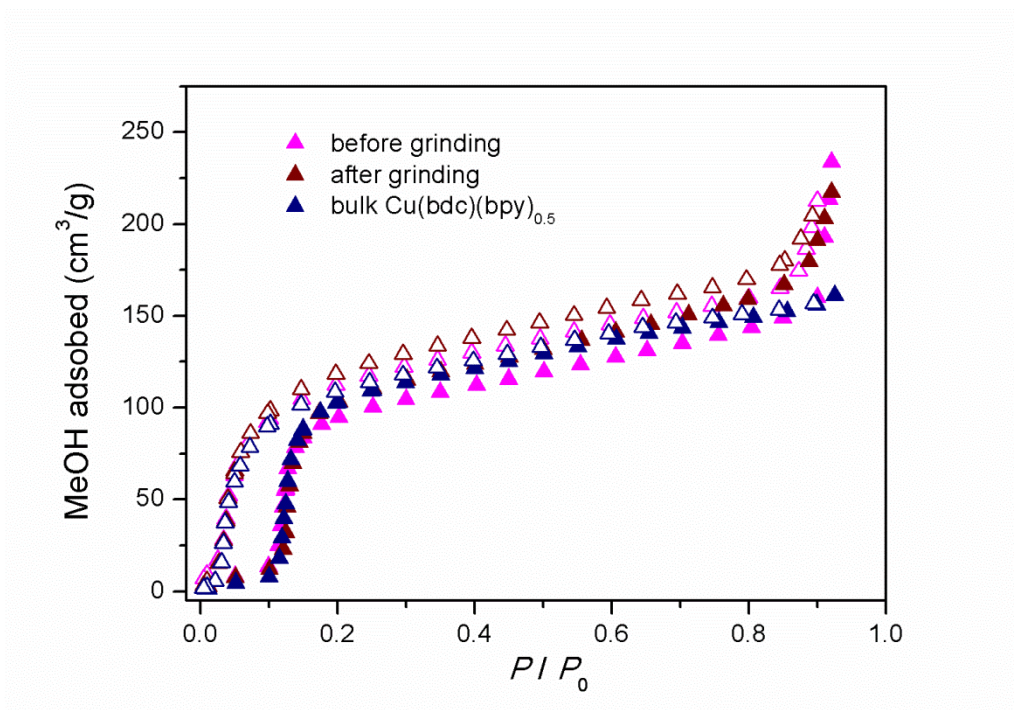


Fig. S15 MeOH adsorption data collected at 298 K for the $\text{Cu}_2(\text{bdc})_2(\text{bpy})$ replicate in monolithic form (pink) and after mechanical grinding (brown), and a bulk $\text{Cu}_2(\text{bdc})_2(\text{bpy})$ sample prepared from $\text{Cu}(\text{OH})_2$ (blue). Closed and open symbols represent adsorption and desorption, respectively.

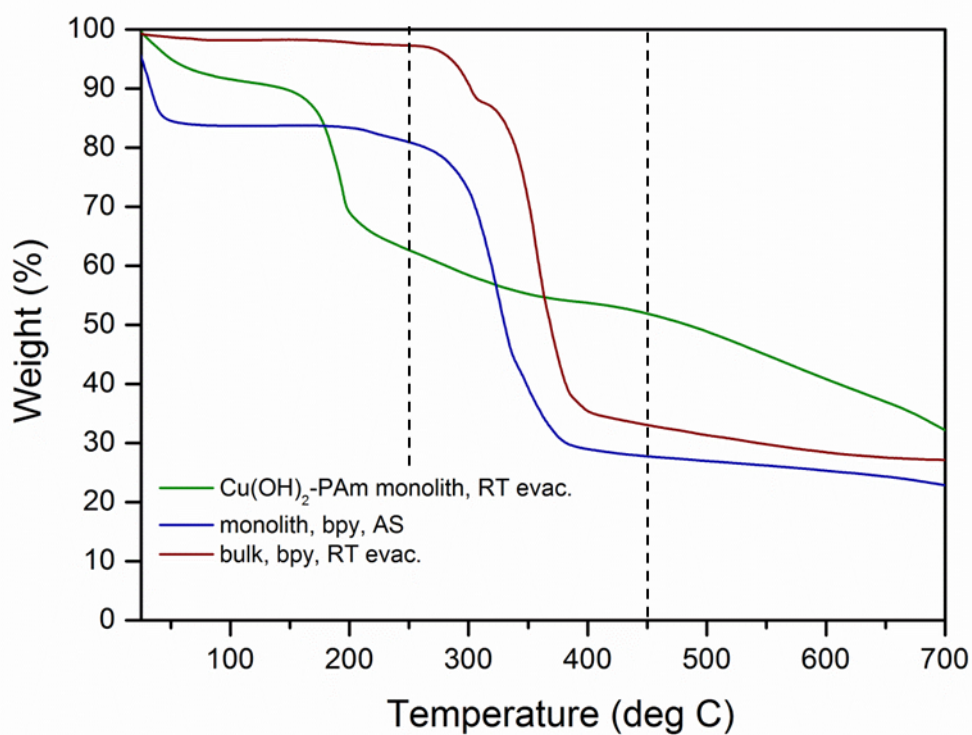


Fig. S16 Thermogravimetric data for the parent Cu(OH)₂-PAAm monolith (green), bulk Cu(bdc)(bpy)_{0.5} (brown), and the Cu(bdc)(bpy)_{0.5}-PAAm monolith (blue) collected under an N₂ flow using a temperature ramp rate of 2 K/min. The dotted line represents the weight transition used to estimate the composition of the replicated monolith.

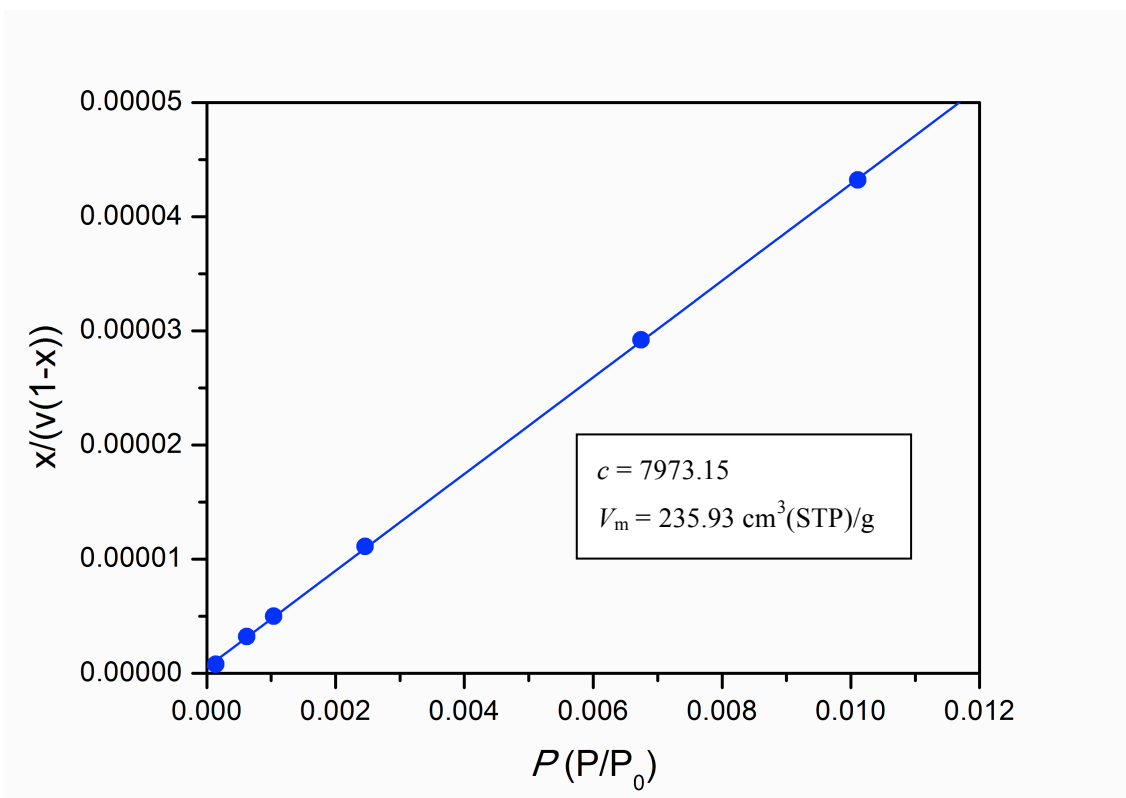


Fig. S17 A BET plot of the adsorption isotherm for N_2 in bulk $\text{Cu}(\text{bdc})(\text{bpy})_{0.5}$ prepared from $\text{Cu}(\text{OH})_2$ at 77 K, where x represents the quantity (P/P_0) and V is the volume of N_2 adsorbed. The blue line represents a linear best fit of the data points. Inset: parameters for the linear best fit and resulting constants for calculation of the BET surface area.

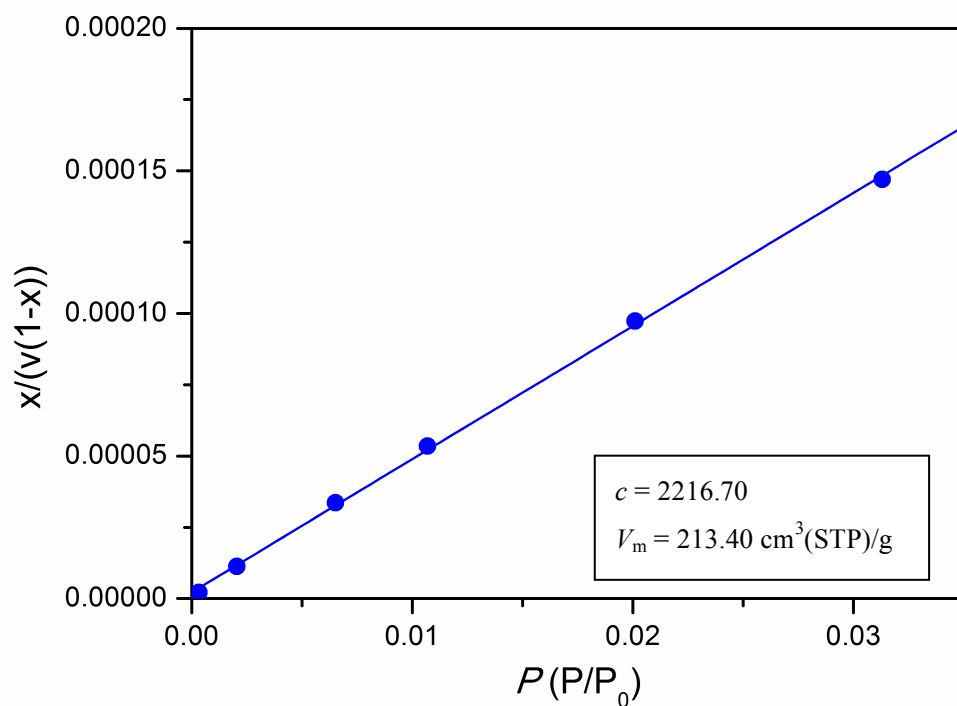


Fig. S18 A BET plot of the adsorption isotherm for N_2 in the $\text{Cu}(\text{bdc})(\text{bpy})_{0.5}\text{-PAAm}$ monolith at 77 K, where x represents the quantity (P/P_0) and V is the volume of N_2 adsorbed. The blue line represents a linear best fit of the data points. Inset: parameters for the linear best fit and resulting constants for calculation of the BET surface area.

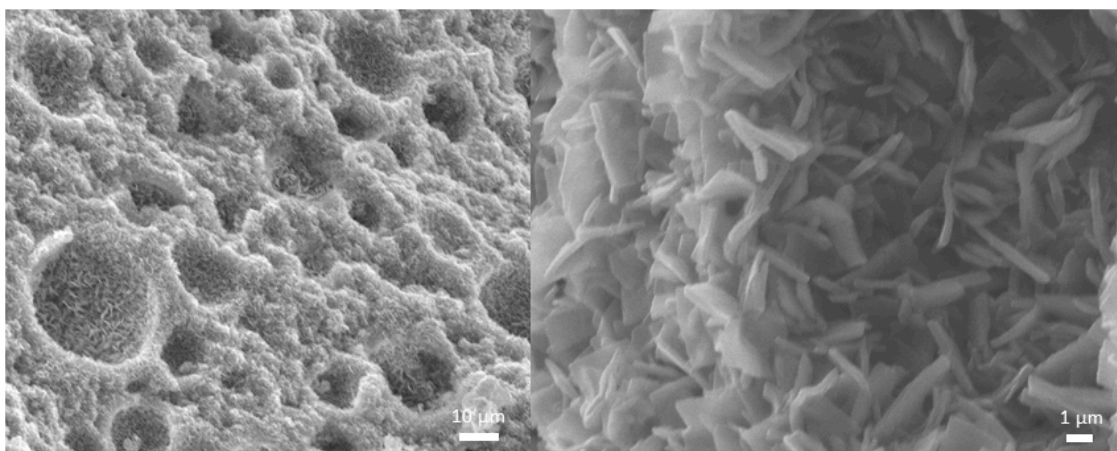


Fig. S19 Field-emission SEM images showing the $\text{Cu}_2(\text{bdc})_2(\text{bpy})$ monolith after evacuation-adsorption-evacuation cycling.

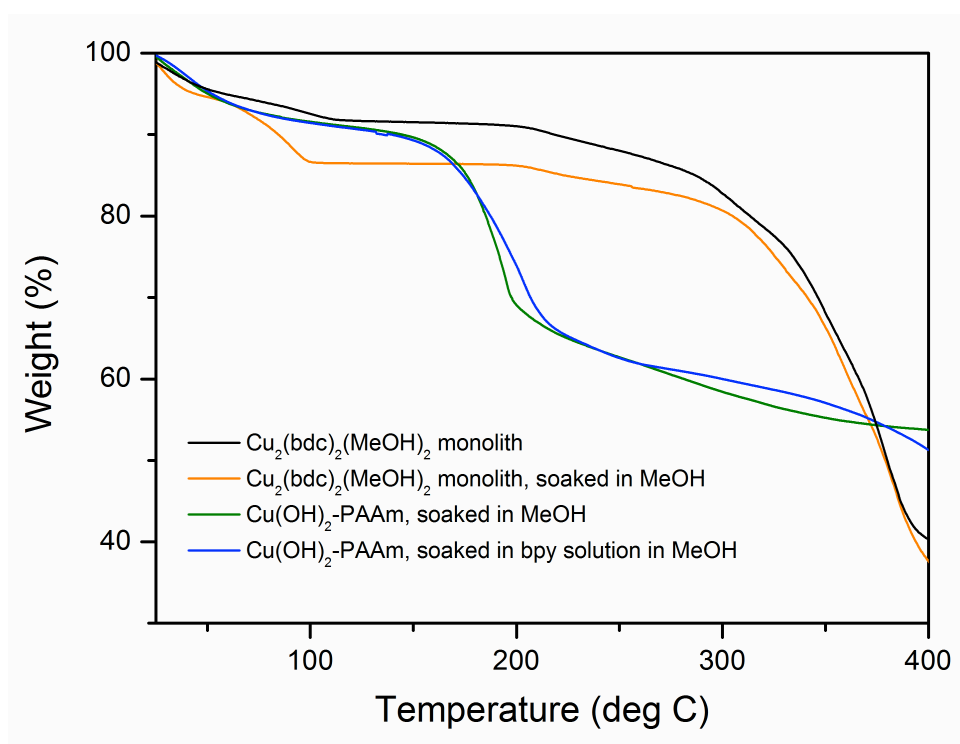


Fig. S20 TGA data for a $\text{Cu}_2(\text{bdc})_2(\text{MeOH})_2$ monolith (black) and after soaking in methanol for 2 weeks (orange), and the $\text{Cu}(\text{OH})_2$ -polyacrylamide monolith soaked in methanol for 2 weeks (green) and in a bpy solution in methanol (blue). Data collected at a ramp rate of 2 K/min.